

1

Introduction

1.1 Exposition

Charged particle dynamics deals with the motion of charged particles in electric and magnetic fields. More specifically, it implies the behavior of *free* charged particles in applied electric and magnetic fields (single-particle dynamics) or in the collective fields generated by the particle distribution if the density is high enough that the mutual interaction becomes significant (self-field effects). Many aspects of gas discharges and plasmas (microscopic motion) are also included in charged particle dynamics. The interaction of free particles with the electron shell of atoms or molecules or with the periodic electric potential of crystals (electron diffraction) as well as the physics of *bound* particles (solid-state theory) are excluded. The particles' behavior in these cases is described by quantum mechanics, not classical mechanics.

The electric and magnetic fields may be static or time dependent and the kinetic energy of the particles may be relativistic. In general, the particles will be treated as classical point charges. Quantum-mechanical effects may be of importance in some applications, for example, in determining the resolution of the electron microscope, but they are ignored in this book. We shall also neglect electromagnetic radiation by accelerated charged particles except for a brief treatment in connection with radiation cooling: *Synchrotron radiation* limits the achievable kinetic energy in circular accelerators, especially for electrons and positrons, but it can also be utilized in damping rings to *cool* these *lepton* beams, as discussed at the end of Chapter 6. On the other hand, we consider collisional effects, such as intrabeam scattering, and collisions between beam particles and gas molecules. They play a major role in charge neutralization due to collisional ionization of the background gas, discussed in Chapter 4; in the formation of the thermal equilibrium distribution, treated in Chapter 5; and as a cause of emittance growth, covered in Chapter 6.

When the self fields are taken into account, a charged particle beam behaves like a *nonneutral* plasma, that is, a special class of plasma having a drift velocity much greater than the random thermal velocity and lacking in general the charge neutrality of a regular plasma composed of particles with opposite charge. A *beam*

is a well-defined flow of a continuous stream or a bunch of particles that move along a straight or curved path, usually defined as the *longitudinal* direction, and that are constrained in the transverse direction by either applied focusing systems or by self-focusing due to the presence of particles with opposite charge. The transverse velocity components and the spread in longitudinal velocities are generally small compared to the mean longitudinal velocity of the beam. Examples are the *straight* beams in linear accelerators, cathode ray tubes, or electron microscopes and the *curved* beams in circular accelerators, such as betatrons, cyclotrons, and synchrotrons.

Most particle accelerators employ radio-frequency (rf) fields to accelerate the particles. The beam in these cases consists of short bunches with a pulse length that is usually small compared with the rf wavelength. To prevent the bunch from spreading due to its intrinsic velocity distribution or due to space-charge repulsion, external focusing forces must be provided in both transverse and longitudinal directions. In rf accelerators, the axial component of the electric field provides focusing in the longitudinal direction, while magnetic fields must be used for transverse focusing. Throughout most of this book we deal with continuous, or *long*, beams and *linear* transverse focusing systems in which the external force on a particle is proportional to the displacement from the axis, or central orbit, of the beam. A brief introduction to the acceleration and focusing of bunched beams is given in Chapter 5.

Nonlinear beam optics, or more generally, nonlinear beam dynamics, which deals with the effects of nonlinear forces due to aberrations in the applied focusing systems, is a highly specialized field that cannot be treated comprehensively within the scope of a book like this. We therefore limit this topic to brief discussions of aberrations in axisymmetric lenses (Section 3.4.6), resonances in circular accelerators (Section 3.8.6), and nonlinear longitudinal beam dynamics in rf accelerators (Section 5.4.8). We do, however, analyze in some detail the generally nonlinear nature of space-charge forces in the thermal distribution, which provides a realistic description of the behavior of laboratory beams (Sections 5.4.4 to 5.4.7 and 6.2). An example of the nonlinear interaction between the aberrations of a solenoid lens and the space charge of an electron beam is presented in Section 5.4.12.

Overall, the material presented in our book is developed in a systematic, largely self-contained manner. We start, in Chapter 2, with a review of the basic principles and formalisms of classical mechanics as applied to charged particle dynamics; our treatment is more comprehensive than the usually brief discussions presented in other books. We then proceed to a broad, general review of beam optics and focusing systems in Chapter 3. The topic of periodic focusing is treated in some detail because of its importance to beam transport and particle accelerators.

A central theme is the role of space charge and emittance in high-intensity, high-brightness beams. In Chapter 4 we use the model of a uniform-density beam with linear self fields. This model allows us to extend the linear beam optics of Chapter 3 to include space charge without having to cope with the mathematically more complicated nonlinear forces. Special emphasis is given to periodic beam trans-

port with space charge (Section 4.4), space-charge effects in circular accelerators (Section 4.5), and charge-neutralization effects (Section 4.6).

The self-consistent theory is developed systematically in Chapter 5 from laminar beams (Section 5.2) to the Vlasov model for beams with momentum spread (Section 5.3), and then to the Maxwell–Boltzmann distribution, which is treated very extensively in Section 5.4. The latter section represents an attempt to develop a unifying thermodynamic description of a beam and contains a considerable amount of new material that is not found in other books on charged particle beams.

The thermodynamic description is continued in Chapter 6, which deals with the fundamental effects causing emittance growth. The concept of free energy, created when a beam is not in equilibrium, and its conversion into thermal energy and emittance growth is treated in Section 6.2, which includes a comparison between theory, simulation, and experiment. Transverse beam modes and instabilities are reviewed in Section 6.3.1. Longitudinal space-charge waves are discussed in Section 6.3.2 since they are fundamental to an understanding of the behavior of perturbations in a beam. Two historically important illustrations of the destructive interaction between the space-charge perturbations and the beam's environment are selected. One is the *resistive wall instability* (Section 6.3.2) in straight systems (microwave devices, linear accelerators); the other is the *longitudinal instability* in circular machines due to *negative-mass* behavior and interaction with the wall represented by a complex impedance (Section 6.3.3). These cases, which are treated for pedagogical reasons on a fundamental level, are intended merely as two examples of the many instabilities that may limit the beam intensity and cause emittance growth. A more extensive discussion of waves and instabilities in beams, including wakefield effects at relativistic energies, is beyond the scope of this book. An excellent introduction and survey of these topics with a comprehensive list of references to the scientific literatures is provided by Lawson [C.17, Chap. 6]. Collective instabilities in high-energy accelerators are treated comprehensively and on an advanced level in terms of the beams' wakefields and the wall impedances in the book by Chao [D.11].

Coulomb collisions as a source of emittance growth and energy spread are treated in Section 6.4. Our analysis of the *Boersch effect* (Section 6.4.1) shows that *intrabeam scattering* is relevant not only in high-energy storage rings (Section 6.4.2) but may also be significant in low-energy beam focusing, transport, and acceleration devices. Scattering in a background gas is discussed in Section 6.4.3. As a natural, complementary addition to our review of emittance growth, we present in Section 6.5 a brief survey of the methods to reduce emittance (*beam cooling*) in storage rings. Finally, in Section 6.6, we summarize the key topics that were discussed, comment on some questions that were left open, and mention a few issues that need further research.

The application of the theory to the design of charged particle beams is stressed throughout the book. Many formulas, scaling laws, graphs, and tables are presented in the text to aid the experimentalists and the designers of charged particle beam devices. Similarly, many of the problems at the end of the chapters were chosen to be of practical interest. The main emphasis of this book, though, is on

the physics and design of *beams*. Only those features of a particular device that are relevant to an understanding of the physics and/or necessary for theoretical analysis and design are treated. Some supplemental material is presented in the appendixes.

Charged particle dynamics and the theory of charged particle beams combine aspects of classical mechanics, electromagnetic theory, geometrical optics, special relativity, statistical mechanics, and plasma physics. A few selected texts covering these fields are listed in the bibliography at the end of the book.

1.2

Historical Developments and Applications

Historically, the first and most prominent area of charged particle dynamics is the field of electron optics, where most of the early work and theoretical development took place and which is well documented in many books listed in part C of the bibliography. The birth of electron optics may be traced to 1926, when H. Busch showed that the action of a short axially symmetric magnetic field on electron rays was similar to that of a glass lens on light rays. Then in 1931 and 1932, Davidson and Calbrick, Brüche, and Johannson recognized that this is also true for axially symmetric electric fields. The first use of magnetic lenses was by Knoll and Ruska (1931) and of electric lenses by Brüche and collaborators (1934).

Up to 1939, electron optics experienced a rapid development stimulated by strong industrial needs, especially electron microscopes, cathode ray tubes, and television. The classic book, which is an encyclopedia of electron optics in this important period and even today is very useful, is that of Zworykin et al., *Electron Optics and the Electron Microscope* [C.1].

During World War II, electron optics received new impulses from war requirements: cathode ray tubes for radar and image-converter tubes for infrared vision, but most important, the development of microwave devices (klystron, magnetron, etc.) for the generation of high-power electromagnetic waves in the range above 1000 MHz. The need for improvement of these latter tubes stimulated interest and progress in the study of space-charge effects in high-intensity beams. The classic reference here is Pierce's book [C.3].

Another important impetus that significantly expanded the field of electron optics, or charged particle dynamics in the broader sense, came from the development of high-energy particle accelerators. This development started around 1930 with the invention of the linear accelerator and the betatron in 1928, the cyclotron in 1931, and the electrostatic accelerator in 1931–1932. This was followed by the large high-energy accelerators existing today, such as the two-mile electron linac at Stanford and the proton synchrotron at Fermilab, near Chicago, now operating at an energy of about 1 TeV and called the *tevatron*. Beam dynamics in particle accelerators is now a major branch of charged particle dynamics. Electron and ion optics was extended to include the focusing of beams in circular accelerators. New types of focusing systems, such as quadrupole lenses, edge focusing in sector-shaped mag-

nets, alternating-gradient focusing, and so on, were invented and contributed to the successful development of accelerators with steadily increasing energies and improving performance characteristics. New interest in particle dynamics came also from space science, industrial applications of electron–ion beam devices (welding, micromachining, ion implantation, charged particle beam lithography), and thermonuclear fusion.

In the decade from 1965 to 1975 two new types of accelerator were developed for the generation of electron beams with high peak power and short pulse length; these are the relativistic diode and the linear induction accelerator. The former produces intense relativistic electron beams (IREB), with peak currents ranging from kiloamperes to mega-amperes and energies from hundreds of keV to more than 10 MeV. Such high-intensity electron beams are created when short high-voltage pulses from so-called *Marx generators* or pulse transformers impinge on the diode. The associated high electric fields cause field emission from the cathode and plasma formation. The plasma expansion leads to gap closure, which, in turn, limits the beam pulse length to between 10 and 100 nanoseconds. These pulsed-power IREB generators have found applications as strong x-ray sources, for studies of the collective acceleration of positive ions by the electric fields associated with intense electron beams, and for the generation of high-power microwaves and *free electron lasers*. More recently, pulsed diodes have been developed that produce high-power ion beams for research on inertial fusion. Miller's book [C.18] presents a very useful introduction to the physics and technology of such pulsed-power, intense particle beams.

Like the betatron, the linear induction accelerator uses inductive electric fields produced by the time-varying flux in magnetic cores. These fields are applied in a sequence of gaps to accelerate pulsed beams of charged particles. The charged particles traverse the gaps only during the time interval in which the magnetic flux is changing, and hence a voltage drop appears across the gaps. In contrast to the radiofrequency resonance accelerators, induction linacs can accelerate very high peak currents, ranging typically from several hundred amperes to several kiloamperes. The largest accelerator in this class was the Advanced Test Accelerator (ATA) at the Lawrence Livermore National Laboratory. It accelerated a 10-kA 70-ns electron beam to an energy of 47 MeV. Originally developed for relatively short electron beams (10 to 100 ns), induction linacs are now also being used for longer pulses (microseconds) of both electron and ion beams. The best example in the latter category is the ion induction linac being developed at the Lawrence Berkeley Laboratory. It is designed for acceleration of high-current heavy-ion beams with the aim of using them as drivers – like laser beams – to ignite the fuel pellets of future inertial fusion reactors. Present experiments are at relatively low energies of a few MeV and a current of $\lesssim 1$ A. A full-scale heavy-ion fusion driver system would require currents of heavy ions (mass number $\gtrsim 100$) in the range 20 to 30 kA with an energy of 5 to 10 GeV and a pulse length of about 10 ns.

The more traditional radio-frequency (rf) linear accelerators are also being developed for high-power applications such as heavy-ion fusion, electron–positron linear colliders for high-energy physics, and other purposes. The invention of

the low-energy radio-frequency-quadrupole (RFQ) accelerator by Kapchinsky and Teplyakov in 1970 has revolutionized the field of rf linacs for ion beams. Today, practically all rf linacs in major laboratories and industry throughout the world use the RFQ as an injector.

Other recent developments involve the use of intense electron beams as electromagnetic radiation sources. Of particular interest in this regard is the gyrotron, a new high-power microwave source in the centimeter and millimeter range, and the free electron laser (FEL), which covers a very wide spectrum from centimeter to optical wavelengths. All of these applications have triggered new research in the physics of intense high-brightness charged particle beams such as transport through periodic-focusing systems, beam stability in the presence of high space-charge forces, interaction with a plasma background, and nonlinear effects responsible for beam deterioration (emittance growth) or particle loss.

This book deals primarily with the theory and design of charged particle beams, not with the design principles of accelerators and other devices which are found in many of the books listed in the bibliography. Thus it will be appropriate to close this historical review by highlighting some of the major early milestones in the development of charged particle beam physics with regard to the theoretical understanding and modeling of the effects of space charge.

The recognition that there are fundamental current limits in charged particle beams plays an important role in beam theory and design. Historically, the fact that the magnetic self field of a relativistic, charge-neutralized beam stops the propagation of the beam when the current exceeds a critical value was discovered by Alfvén (in 1939) for electron propagation through space and later applied to laboratory beams by Lawson (in 1958). The critical current associated with this effect is known in the literature as the *Alfvén current* or *Alfvén–Lawson current*. Closely related to this effect is the work on self-focused relativistic electron beams by Bennett (1934) and Budker (1956).

The current limit due to space charge (in the absence of charge neutralization) in a diode is known as the *Child–Langmuir law* and dates to the early work of Child (1911) and Langmuir (1913). However, the related limit for a beam propagating through a drift tube was studied much later, and the formula for a relativistic electron beam derived by Bogdankevich and Rukhadze in 1971 is probably the one cited most frequently in the literature.

The foundation for the mathematical treatment of beams with space charge was laid by Vlasov in 1945. Vlasov integrated Liouville's theorem, Maxwell's equations, and the equations of motion into a self-consistent theoretical model that has become an indispensable tool for the theoretical analysis of beams. In 1959, Kapchinsky and Vladimirskey proposed a special solution to the Vlasov equation, known in the literature as the *K–V distribution*, which has the property that the transverse space-charge forces are linear functions of the particles' positions in the beam. This was a major milestone in beam physics whose practical importance for analysis and design cannot be overemphasized. The K–V distribution gained additional significance when Lapostolle and Sacherer in 1971 introduced the description of beams in terms of the root-mean-square (rms) properties (rms width, divergence,

and emittance). They showed that beams having the same rms properties are equivalent. This equivalency principle is used extensively in Section 5.4 for correlating the nonanalytical Maxwell–Boltzmann distribution with the analytical K–V distribution in the transverse direction and with the parabolic line-charge distribution in the longitudinal direction, and in Section 6.2 for our theoretical treatment of emittance growth.

Another important milestone in the development of beam physics is the detailed pioneering work by Laslett in 1963 on the space-charge tune shift of the betatron oscillations in circular accelerators. This effect, often referred to as the *Laslett tune shift*, is of fundamental importance, as it limits the achievable intensity in these machines. With regard to understanding the physics of space-charge-dominated beams, the simulation work by Chasman in 1968 for linear accelerators, the analysis of collective oscillation modes in uniformly focused beams by Gluckstern, and the stability analysis by Davidson and Krall in 1970 constitute important achievements which influenced future work.

This list of historical milestones is obviously quite subjective and incomplete and could be extended into many directions, such as the rich field of beam instabilities, where the theoretical analysis of the *negative-mass instability* in 1959 comes to mind as a major event. But this book is not about instabilities. Furthermore, we wanted to limit the list to “historical” milestones, defined somewhat arbitrarily as events that occurred more than 20 years ago.

1.3

Sources of Charged Particles

Although the main topic of this book is beam dynamics, it will be beneficial to review briefly the basic principles and performance limitations of typical particle sources. This is particularly important for intense beams, where physical and technological constraints of the source pose fundamental limits for the beam current and the emittance or brightness that can be achieved.

The simplest conceptual model of a source is the planar diode. One of the two electrodes emits the charged particles; in the case of electrons it is called a *cathode*. A potential difference of the appropriate polarity accelerates the particles to the other electrode, called the *anode* in the electron case. In practice, the emitter has, of course, a finite size, and usually a circular shape with radius r_s . The *anode* contains a hole or a mesh to allow the beam to propagate into the vacuum tube downstream, where it is focused or accelerated depending on the particular application. Furthermore, the electrode in which the emitter is embedded as well as the *anode* may have a special nonplanar design to provide initial focusing for the beam. In a *Pierce-type* geometry, for example, the electrodes form an angle of less than 90° with respect to the beam axis to produce a transverse electrostatic force that exactly balances the repulsive Coulomb force due to the space charge of the beam (see [C.3, Chap. X]).

A schematic illustration of a typical diode-type electron gun with thermionic cathode, Pierce-type focusing electrode, and anode mesh is shown in Figure 1.1. The

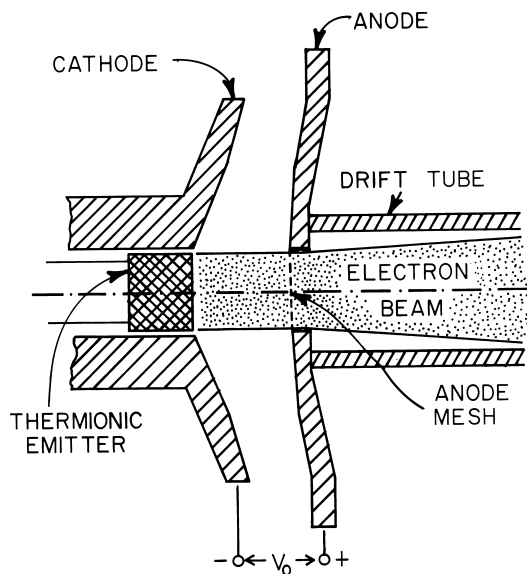


Fig. 1.1 Schematic of an electron gun with thermionic cathode, Pierce-type-electrode geometry, and anode mesh. (See Appendix 1 for a discussion of such a gun without anode mesh.)

electron beam radius in this example remains practically constant within the gun and then increases due to space-charge repulsion when the beam enters the field-free region outside the anode. To prevent divergence due to space-charge forces or transverse velocity spread, the beam has to be focused with appropriate magnetic or electrostatic lenses, as discussed in this book. Other types of electron sources employ field emission or photocathodes; the cathodes may have the shape of an annulus (to form a hollow beam) or a sharp tip. Additional intermediate electrodes (triode or tetrode configurations) may be used to control the beam parameters.

Conduction electrons in a metal have an energy distribution that obeys the Fermi–Dirac statistics. The electrons emitted from a thermionic cathode belong to the *Maxwellian tail* of the Fermi–Dirac distribution, and the current density J_{th} is given by the *Richardson–Dushman equation* [1]

$$J_{\text{th}} = AT^2 e^{-W/k_B T}. \quad (1.1)$$

Here T is the cathode temperature, W the work function of the cathode material (typically a few eV), and k_B is Boltzmann's constant (8.6175×10^{-5} eV/K). The theoretical value for the constant A is

$$A = \frac{4\pi emk_B^2}{h^3} = 1.2 \times 10^6 \text{ Am}^{-2}\text{K}^{-2}, \quad (1.2)$$

where $e = 1.6 \times 10^{-19}$ C is the electron charge, $m = 9.11 \times 10^{-31}$ kg the electron rest mass, and $h = 6.63 \times 10^{-34}$ Js is Planck's constant. Experimentally, one finds a value for A that is lower than (1.2) by a factor of about 2. Fabrication of

thermionic cathodes is a highly specialized art where the choice and composition of materials is guided by requirements of low work function W , long lifetime (at high temperature), smoothness of emitting surface, and other factors. Pure tungsten has a work function of $W = 4.5$ eV, and tungsten cathodes operate at a temperature of 2500 K ($k_B T \sim 0.2$ eV), with a current density of about 0.5 A/cm 2 . Considerably higher current densities of 10 to 20 A/cm 2 can be achieved with dispenser cathodes, which are used for high-power microwave generation. Dispenser cathodes use barium or strontium oxides impregnated in a matrix of porous tungsten (or similar metals). These cathodes operate at a typical temperature of 1400 K ($k_B T \sim 0.12$ eV) and have an effective work function of 1.6 eV.

A typical ion source with a diode configuration is shown schematically in Figure 1.2. The ions are extracted from the plasma of a gas discharge, and the accelerated beam passes through a hole in the *extraction electrode* into the vacuum drift tube. The emitting plasma surface area is not fixed as in the case of a cathode. Rather, it has a concave shape, called *meniscus*, which depends on the plasma density and the strength of the accelerating electric field at the plasma surface. The dashed lines in Figure 1.2 indicate the equipotential surfaces of the electric field distribution due to the applied voltage V_0 as well as the space charge of the beam. Note that there is a small potential drop between the plasma surface and the wall of the chamber that encloses the plasma. The concave shape of the meniscus and the aperture in the source electrode produce a transverse electric field component that results in a converging beam.

In general, ion sources are much more complex than electron guns. There are many different types of sources for the various particle species, such as light ions, heavy ions, or negative ions (e.g., H $^-$). Most of the sources employ magnetic fields to confine the plasma. Some have several electrodes at different potentials to better control the ion beam formation and acceleration process. A special problem with ion sources is the gas in which the plasma is formed and which leaks through the source aperture into the acceleration gap and the drift tube. Near the source the pressure is high enough that a plasma with density exceeding the beam density can be formed through ionizing collisions between the beam ions and gas molecules. This causes space-charge neutralization, which is advantageous for focusing but may also cause detrimental effects such as high-voltage breakdown and beam plasma instabilities. Another problem arises because ions with different charge state or mass are extracted from the plasma together with the desired species. In the case of negative ions such as H $^-$, for instance, electrons are also accelerated with the ion beam. Unless the number of contaminating particles is small, it is necessary in these cases to use deflecting magnetic fields to remove the undesired particle species from the beam.

For our purpose of illustrating the basic design concept of charged particle sources it suffices to consider the simple diode configurations of Figures 1.1 and 1.2. In such sources the space-charge electric field limits the amount of current that can be accelerated by a given voltage V_0 . For a planar electrode geometry with

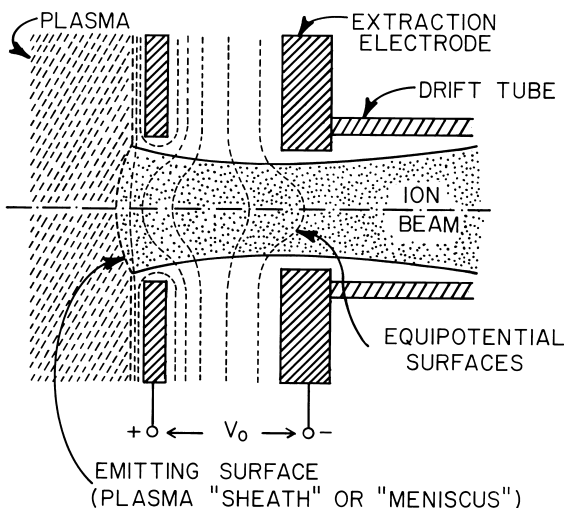


Fig. 1.2 Schematic of a plasma ion source. The equipotential surfaces of the electric field distribution are indicated by dashed lines. The ions are emitted from the concave plasma sheath, which forms an equipotential surface.

a gap spacing d between the two plates, the limiting current density J (in the non-relativistic limit and in MKS units) is given by the formula

$$J = 1.67 \times 10^{-3} \left(\frac{q}{mc^2} \right)^{1/2} \frac{V_0^{3/2}}{d^2} \quad [\text{A/m}^2], \quad (1.3)$$

where q and m are the particle charge and mass, respectively, and c is the speed of light. The relation, first derived by Child and Langmuir [2], is known in the literature as *Child's law* or as the *Child-Langmuir law*. Applying this result to a uniform round beam emitted from a circular area with radius r_s yields for the beam current

$$I = 1.67\pi \times 10^{-3} \left(\frac{q}{mc^2} \right)^{1/2} V_0^{3/2} \left(\frac{r_s}{d} \right)^2 \quad [\text{A}]. \quad (1.4)$$

However, in practical ion sources and electron guns with cylindrical geometry the beam current may be considerably lower than this limit, which is based on an ideal one-dimensional planar-diode geometry. The ratio $I/V_0^{3/2}$ is known as the *perveance* of the beam. A derivation of Child's law is given in Section 2.5.2.

An important figure of merit for a high-brightness beam is the *emittance*, which is basically defined by the product of the width and transverse velocity spread of the beam. The electrons in the tail of the Fermi-Dirac distribution inside a cathode and the ions in the plasma source have a Maxwellian velocity distribution given by

$$f(v_x, v_y, v_z) = f_0 \exp \left[- \frac{m(v_x^2 + v_y^2 + v_z^2)}{2k_B T} \right], \quad (1.5)$$

where T is the temperature of the cathode or the plasma. As a result, the particles emerge from the source with an intrinsic velocity spread. If x and y denote the two

cartesian coordinates perpendicular to the direction of the beam, the rms values of the transverse velocity spread for the Maxwellian distribution are readily found to be

$$\tilde{v}_x = \tilde{v}_y = \left(\frac{k_B T}{m} \right)^{1/2}. \quad (1.6a)$$

If the emitting surface is a circle with radius r_s and with uniform current density, the rms width of the beam is

$$\tilde{x} = \tilde{y} = \frac{r_s}{2}. \quad (1.6b)$$

As explained in Section 3.2, an *effective normalized emittance* is defined nonrelativistically as

$$\epsilon_n = 4\tilde{x} \frac{\tilde{v}_x}{c} \quad (1.7a)$$

Substitution of (1.6a) and (1.6b) in (1.7a) yields

$$\epsilon_n = 2r_s \left(\frac{k_B T}{mc^2} \right)^{1/2} \quad [\text{m-rad}]. \quad (1.7b)$$

The normalized emittance measures the beam quality in two-dimensional *phase space*, which is defined by the space and momentum coordinates of the particle distribution (i.e., x , p_x , or x , v_x , nonrelativistically). From Liouville's theorem (discussed in Section 3.2) it may be shown that the normalized emittance remains constant if there are no nonlinear forces or coupling forces between different coordinate directions. Thus Equation (1.7b) constitutes a lower theoretical limit; in practice, nonlinear beam dynamics, instabilities, and other effects may cause emittance growth, so that the actual value is always larger than (1.7b).

For many high-power applications the output current of an electron gun is limited by the achievable current density J_c at the cathode rather than by the space-charge limit and by the high-voltage breakdown effect to be discussed below. In the widely used thermionic cathodes, current densities, in practice, are normally limited to 10 to 20 A/cm², and values as high as 100 A/cm² have been achieved in experimental studies, depending on the desired cathode lifetime, average beam power, and other factors. If the current density J_c is fixed, the desired beam current I determines the cathode radius r_s and hence also the emittance ϵ_n . Using $r_s = (I/J_c\pi)^{1/2}$, one can write Equation (1.7b) in the form

$$\epsilon_n = 2 \left(\frac{I}{J_c\pi} \right)^{1/2} \left(\frac{k_B T}{mc^2} \right)^{1/2} \quad [\text{m-rad}], \quad (1.8)$$

which shows that the emittance increases with the square root of the product of beam current and cathode temperature and decreases with current density as $J_c^{-1/2}$. For $J_c = 10 \text{ A/cm}^2 = 10^5 \text{ A/m}^2$ and $k_B T = 0.1 \text{ eV}$, one obtains $\epsilon_n = 1.6 \times 10^{-6} I^{1/2} \text{ m-rad}$.

In a new type of electron gun with photocathode that is being developed at various laboratories, a high-power laser beam is focused on the cathode surface and

electron currents of several hundred A/cm² have been achieved. The photocathode is located inside the first cavity of an rf injector-linac structure, as shown in Figure A5.1 of Appendix 5. The strong axial electric field in this cavity (20–100 MV/m) rapidly accelerates the electrons to a high-energy ($\gtrsim 1$ MeV). Timing and length of the laser pulse are chosen to produce a short electron bunch during a small phase interval within the accelerating part of the rf cycle. The high-brightness beams produced by the laser-driven *rf photocathode guns* are of particular interest for advanced particle accelerator applications such as high-energy e⁺e⁻ linear colliders and free electron lasers (FELs), which require beams with high intensity but very small emittance. The rf photocathode gun was first developed at Los Alamos, and the general concept is described in the early papers by Fraser et al. [3]. More recent reviews of the developments in this field can be found in References [4] and [5]. The problem of emittance growth in such electron guns due to rf defocusing and nonlinear space-charge forces is discussed briefly in Appendix 5.

The above scaling does not apply for high-intensity plasma-type ion sources with a simple diode geometry. In this case the achievable beam current is often limited by Child's law and by high-voltage breakdown. Several different empirical formulas for voltage breakdown have been developed over the years based on practical experience and theoretical models. According to these formulas the gap width d between the electrodes must not be smaller than a critical value that depends on the voltage V_0 between the electrodes as

$$d = CV_0^\alpha, \quad (1.9)$$

where C is a constant and the exponent α ranges between $1 < \alpha < 2$, depending on the model for breakdown. In one model, the electric field strength, V_0/d , is the parameter controlling breakdown, hence $\alpha = 1$. Another model assumes that the product of field strength and gap voltage (i.e., V_0^2/d) determines the breakdown condition, so that $\alpha = 2$. In a recent survey of experimental results with ion sources, Keller concluded that the relation

$$d[\text{mm}] = 1.4 \times 10^{-2} V_0^{3/2} [\text{kV}] \quad (1.10)$$

(i.e., $\alpha = 1.5$) provided the best fit to the data [4]. This appears to be a reasonable compromise between the two extreme cases of $\alpha = 1$ and $\alpha = 2$. It should be pointed out, however, that such simple scaling laws have to be used with some caution. In practice, electrical breakdown is a very complicated phenomenon that depends on many details (other than gap spacing and voltage), such as gas flow from the source, geometry of the electrode structures, and surface cleanliness.

Another important constraint influencing the output characteristics (perveance and emittance) of high-current, low-emittance charged particle sources is imposed by considerations of beam optics. To minimize nonlinearities in the electrostatic field configuration, especially spherical aberrations, which would adversely affect the beam quality, the radius r_s of the beam at the emitter surface must not be larger than the gap width d . In most high-perveance ion source designs, for instance, the ratio r_s/d is in the range

$$0.2 < \frac{r_s}{d} < 1.0. \quad (1.11)$$

It should be noted that this beam optics argument does not apply to intense relativistic electron beams and high-power ion diodes producing charge-neutralized beams with intensities far above the space-charge limit given in Equation (1.4).

The above set of equations and constraints defines the parameter space for high-perveance electron or ion sources. Thus, the intrinsic normalized emittance ϵ_n is determined by the beam radius r_s at the emitter surface and the source temperature $k_B T$ according to Equation (1.7). For electrons from thermionic cathodes, one typically has $k_B T_e \approx 0.1$ eV, while ion temperatures from plasma sources (e.g., protons or H^- ions) are usually an order of magnitude higher (i.e., $k_B T_i \approx 1$ to 5 eV). If ϵ_n , and thus r_s , are given (to meet the requirements of a particular application), the beam current and voltage are defined by Child's law (1.4) and the two constraints imposed by electrical breakdown (1.10) and beam optics (1.11).

For experiments in which a high-intensity beam is to be focused to a small spot size, the *unnormalized emittance* at the final beam energy, $\epsilon = \epsilon_n / \beta \gamma$, which represents the product of beam radius and divergence angle, is an important parameter. It is inversely proportional to the relativistic velocity and energy factors $\beta = v/c$ and $\gamma = (1 - \beta^2)^{-1/2}$, and hence decreases as the particles are accelerated to high energy. Emittance by itself is not sufficient to characterize the beam quality. A better figure of merit is the *brightness* B defined by the ratio of beam current I and the product of the two emittances, i.e., I/ϵ^2 for axisymmetric beams [see Equation (3.8)]. Since the emittance changes with energy, it is preferable to use the *normalized brightness* defined as $B_n = 2I/\pi^2\epsilon_n^2$ [Equation (3.22)]. The normalized brightness, like the normalized emittance ϵ_n , is an invariant in an ideal system. Emittance growth due to nonlinear forces, instabilities, and other effects (discussed in Chapter 6) decreases the normalized brightness. By comparing the actual beam brightness with the ideal value one can assess the effectiveness of the design and performance characteristics of a particular device. As an example, let us consider a high-intensity electron beam from a dispenser-type cathode. Using Equation (1.8), one finds that the normalized brightness has an upper limit of

$$B_n = \frac{J_c}{2\pi} \frac{mc^2}{k_B T}. \quad (1.12a)$$

This brightness limit depends on the ratio of the current density J_c at the cathode and the temperature T of the cathode, and it is independent of the current I . If one operates at a maximum current density of $J_c = 10$ A/cm² and at a cathode temperature of $k_B T = 0.1$ eV, the brightness has an upper limit of

$$B_n = 8 \times 10^{10} \text{ A}/(\text{m}\cdot\text{rad})^2. \quad (1.12b)$$

In practice, the brightness of the electron beam in the system downstream from the electron gun will always be less than this ideal value.

The preceding discussion was intended to provide an introductory overview of basic design principles of charged particle sources and of the fundamental performance limits of high-intensity beams due to constraints imposed by the physics and technology of source operation. Detailed descriptions can be found in the literature, such as the books C.15, C.16, and C.23 listed in the bibliography, and in the

proceedings of accelerator conferences or topical meetings on low-energy beams and sources.

References

- 1 RICHARDSON, O. W., *Phil. Mag.* **28**(5), 633 (1914); DUSHMAN, S., *Phys. Rev.* **21**(6), 623 (1923).
- 2 CHILD, C. D., *Phys. Rev. Ser. I* **32**, 492 (1911); LANGMUIR, I., *Phys. Rev. Ser. II* **2**, 450 (1913).
- 3 FRASER, J. S., SHEFFIELD, R. L., GRAY, E. R., RODENZ, G. W., *IEEE Trans. Nucl. Sci.* **NS-32**, 1791 (1985); FRASER, J. S., SHEFFIELD, R. L., *IEEE J. Quantum Electron.* **23**, 1489 (1987).
- 4 O'SHEA, P., REISER, M., *AIP Conference Proc.* **279**, 579 (1993), ed. WURTELE, J. S.
- 5 BEN-ZVI, I., Conference Record of the 1993 IEEE Particle Accelerator Conference, 93CH3279-7, p. 2964, ed. WURTELE, J. S.
- 6 KELLER, R., "High Current, High Brightness, and High Duty Factor Ion Injectors," *AIP Conf. Proc.* **139**, 1 (1986), ed. GILLESPIE, G., KUO, Y. Y., KEEFE, D., WANGLER, T. P.